Video Article

Plasmonic Trapping and Release of Nanoparticles in a Monitoring Environment

Jung-Dae Kim[1], Yong-Gu Lee[2]

[1]Division of Scientific Instrumentation, Korea Basic Science Institute (KBSI)

[2]School of Mechanical Engineering, Gwangju Institute of Science and Technology (GIST)

Correspondence to: Yong-Gu Lee at lygu@gist.ac.kr

URL: https://www.jove.com/video/55258
DOI: doi:10.3791/55258

Keywords: Engineering, Issue 122, plasmonics, plasmonic tweezers, optical trapping, optical forces, microfluidics, nanohole, immobilization of nanoparticles

Date Published: 4/4/2017

Citation: Kim, J.D., Lee, Y.G. Plasmonic Trapping and Release of Nanoparticles in a Monitoring Environment. *J. Vis. Exp.* (122), e55258, doi:10.3791/55258 (2017).

Abstract

Plasmonic tweezers use surface plasmon polaritons to confine polarizable nanoscale objects. Among the various designs of plasmonic tweezers, only a few can observe immobilized particles. Moreover, a limited number of studies have experimentally measured the exertable forces on the particles. The designs can be classified as the protruding nanodisk type or the suppressed nanohole type. For the latter, microscopic observation is extremely challenging. In this paper, a new plasmonic tweezer system is introduced to monitor particles, both in directions parallel and orthogonal to the symmetric axis of a plasmonic nanohole structure. This feature enables us to observe the movement of each particle near the rim of the nanohole. Furthermore, we can quantitatively estimate the maximal trapping forces using a new fluidic channel.

Video Link

The video component of this article can be found at https://www.jove.com/video/55258/

Introduction

The ability to manipulate microscale objects is an indispensable feature for many micro/nano experiments. Direct contact manipulations can damage the manipulated objects. Releasing the previously held objects is also challenging because of stiction problems. To overcome these issues, several indirect methods using fluidic[1], electric[2], magnetic[3], or photonic forces[4,5,6,7,8] have been proposed. Plasmonic tweezers that use photonic forces are based on the physics of extraordinary field enhancement several orders larger than the incident intensity[9]. This extremely strong field enhancement enables the trapping of extremely small nanoparticles. For example, it has been shown to immobilize and manipulate nanoscale objects, such as polystyrene particles[7,10,11,12,13,14], polymer chains[15], proteins[16], quantum dots[17], and DNA molecules[8,18]. Without plasmonic tweezers, it is difficult to trap nanoparticles because they quickly disappear before they are effectively examined or because they are damaged due to the high intensity of the laser.

Many plasmonic studies have used various nanoscale gold structures. We can categorize the gold structures as protruding nanodisk types[12,13,14,15,19,20,21] or suppressed nanohole types[7,8,10,11,22,23]. In terms of imaging convenience, the nanodisk types are more suitable than the nanohole types because, for the latter, the gold substrates can obstruct the observation view. Moreover, the plasmonic trapping occurs near the plasmonic structure and makes observation even more challenging. To the best of our knowledge, plasmonic trapping on nanohole types was only verified using indirect scattering signals. However, no successful direct observations, such as microscopic images, have been reported. Few studies have described the position of trapped particles. One such result was presented by Wang *et al*. They created a gold pillar on a gold substrate and observed the particle motion using a fluorescent microscope[24]. However, this is only effective for monitoring lateral movements not in the direction parallel to the beam axis.

In this paper, we introduce new fluidic microchip design and fabrication procedures. Using this chip, we demonstrate the monitoring of plasmonically trapped particles, both in directions parallel and orthogonal to the plasmonic nanostructure. Furthermore, we measure the maximal force of the immobilized particle by increasing the fluid velocity to find the tipping velocity in the microchip. This study is unique because most studies on plasmonic tweezers cannot quantitatively show the maximal trapping forces used in their experimental setups.

Protocol

Caution: Please refer to all relevant material safety regulations before use. Several of the chemicals used in microchip fabrication are acutely toxic and carcinogenic. Please use all appropriate safety practices when performing the photolithography and etching processes, including the use of engineering controls (fume hood, hot plate, and aligner) and personal protective equipment (safety glasses, gloves, lab coat, full-length pants, and closed-toe shoes).

1. Fabrication of the PDMS Microchannel

1. Fabrication of the microchannel mold by the photolithograph process
    1. Completely remove foreign substances on the 4-inch Si wafer surface with piranha cleaning (**Figure 1a**). Mix sulfuric acid (H_2SO_4) and hydrogen peroxide (H_2O_2) at a ratio of 3:1 to make the piranha solution in the dish. Mix by gradually adding small amounts of the strong acid (H_2O_2) to the weak acid (H_2SO_4); reversing this order may cause an explosion because of the highly reactive strong acid.
    2. Immerse the wafer in the piranha solution for 10 min. Subsequently, immerse the wafer in deionized (DI) water for 3 min to remove the remaining piranha solution. Rinse the wafer with flowing DI water for 10 s. Repeat the rinsing procedure 3 times and dry with N_2 gas to remove the remaining DI.
    3. Place the wafer on a hot plate for 20 min at 180 °C to further dehydrate the wafer.
    4. Pour 5 mL of the negative photoresist on top of the wafer and spin coat for 45 s at 1,500 rpm (**Figure 1b**); after spin coating, a photoresist bead is created at the wafer edge because of the relatively high viscosity of the photoresist.
    5. Balance the photoresist-coated wafer by planarization on a leveling stand for 5 h.
    6. Place the photoresist-coated wafer on a hot plate for 12 min at 65 °C, 35 min at 95 °C, and 12 min at 65 °C (soft baking).
    7. Fix the film mask on the mask holder and the soft-baked wafer on the substrate stage of the aligner. Expose to ultraviolet (UV) light for 43 s at 650 mJ/cm^2 to solidify the photoresist.
    8. Place the wafer on the hot plate for 5 min at 65 °C, 15 min at 95 °C, and 5 min at 65 °C (post-exposure baking).
    9. Immerse the wafer in the photoresist developer for 30 min to remove unsolidified photoresist.
    10. Rinse the wafer with isopropyl alcohol (IPA) and dry with N_2 gas to remove the remaining IPA.

2. Manufacture of the PDMS microchannel
    1. Treat the surface of the wafer and the photoresist mold for 1 min at a power of 200 W using an atmospheric plasma machine[25]; the gas flows of CH_4 and He should be 6 and 30 sccm, respectively. Perform this hydrophobic treatment to easily detach the polydimethylsiloxane (PDMS) microchannel from the surface of the wafer and photoresist mold (**Figure 1c**).
    2. Prepare the PDMS solution by mixing the PDMS base and curing agent at a ratio of 10:1. Stir the mixture for 2 min.
    3. Place the wafer inside a Petri dish (150 mm x 15 mm) and add 100 mL of the PDMS solution. Remove the bubbles that were created from stirring using a desiccator.
    4. Place the Petri dish in the oven for 2 h at 80 °C to solidify the PDMS solution (**Figure 1d** and **h**).
    5. Cut along the contours of the PDMS microchannel with a razor blade and detach it from the wafer; the fabricated PDMS microchannel should have the following dimensions: 13 mm long, 300 µm wide, and 150 µm high (**Figures 1e**, **f**, and **i**).
    NOTE: Two types of holes are produced by a micropuncture to insert the single-mode fiber (SMF) cable and the tubes (inlet and outlet) on the PDMS microchannel (**Figure 1g**). The SMF cable is used to emit the laser beam to the nanohole milled on the gold plate. The tube is used to insert/extract the particle solution to/from the PDMS microchannel.
    6. Puncture 1.5-mm inlet and outlet holes at each end of the PDMS microchannel. Puncture a 0.3-mm SMF cable hole at the center of the PDMS microchannel.

2. Etching Process of the Gold Plate

1. Prepare a commercially available gold plate with the dimensions of 25 x 6.25 mm^2 (**Figure 2a**).
2. Remove any foreign substances on the gold plate with the following cleaning procedures. Clean in the following order by immersing in acetone, methanol, and DI water for 5 min each.
3. Rinse the gold plate 3 times with DI water for 10 s and dry the plate with N_2 gas to remove the remaining DI water.
4. Place the gold plate on a hot plate for 20 min at 180 °C to completely remove any remaining moisture.
5. Pour 0.5 mL of hexamethyldisilazane (HMDS) on the gold plate and spin coat for 40 s at 3,000 rpm.
6. Pour 0.5 mL of positive photoresist on top of the spin-coated HMDS and spin coat for 40 s at 3,000 rpm (**Figure 2b**).
7. Place the photoresist-coated gold plate on the hot plate for 90 s at 110 °C (soft baking).
8. Fix the film mask on the glass wafer and place the soft-baked gold plate on the substrate stage. Expose to UV light for 4.5 s at 64 mJ/cm^2 to dissolve the photoresist.
9. Immerse the gold plate in the photoresist developer for 1 min to remove the dissolved photoresist (**Figure 2c**). Rinse the gold plate with DI water and dry with N_2 gas.
10. Immerse the gold plate in the Au etchant for 45 s at an etching rate of 28 Å/s to remove the exposed Au (**Figure 2d**). Rinse the gold plate with DI water and dry with N_2 gas.
11. Immerse the gold plate in the Ti etchant for 5 s at an etching rate of 25 Å/s to remove the exposed Ti (**Figure 2e**). Rinse the gold plate with DI water and dry with N_2 gas.
12. Remove the remaining photoresist on the gold plate by immersing it in acetone, methanol, and DI water for 3 min each (**Figure 2f**); immerse the plate in the written order.
13. Rinse the gold plate 3 times with DI water for 10 s. Dry with N_2 gas to remove the DI water.
14. Place the gold plate on the hot plate for 3 min at 120 °C to completely remove the moisture; the produced gold block should be 400 x 150 µm^2 (**Figure 2h**).
15. Mill a 400-nm nanohole using a focused ion beam (FIB) at the center of the gold block that was fabricated after etching (**Figures 2g** and **i**). Create a 370-nm circle pattern to focus on the gold block with an ion accelerating voltage of 30 kV at 28 pA for 3 s.

3. Assembly of the Microchip

1. Treat the two surfaces of the PDMS microchannel and gold plate for 1 min with O_2 plasma to attach them together with a plasma system at a power of 80 W and a pressure of 825 mTorr[25].

NOTE: It is notably difficult to attach them with precision because the gold block and PDMS microchannel are on the micrometer level. Hence, use an aligner with a camera and a manual stage.

2. Fix the glass wafer that is used to attach the film mask to the mask holder of the aligner (**Figure 3a**).
3. Attach the O_2-plasma-treated PDMS microchannel to the glass wafer; because the PDMS is hydrophilic, it will easily attach to the glass wafer without any adhesion solution. Fix the gold plate on the substrate stage of the aligner (**Figure 3a**).
4. Locate the centers of the SMF cable hole and gold block, which are aligned on the same axis, using the camera on the aligner. Lift the manual stage to combine the two parts (**Figures 3b** and **c**).

4. Improvement of the Microchip Side Surface Roughness by PDMS Coating

NOTE: The gold plate with fixed dimensions of 400 x 150 μm^2 is relatively more difficult to cut out than the PDMS material. Therefore, to detach the PDMS microchannel from the wafer, a razor blade is used to cut out a larger piece than the gold plate. After combining the two parts, the excess parts of the PDMS relative to the gold plate must then be cut so that the inside of the channel can be observed from the side using a microscope (**Figure 4a**). However, the cut surface, which is used as a window, has a high surface roughness and consequently produces cloudy images of the particles that flow in the channel (**Figure 4b**). Coating with the PDMS solution is performed again to resolve this problem.

1. Prepare the PDMS solution by mixing the PDMS base and curing agent at a 10:1 ratio and stir for 2 min.
2. Pour 2 mL of the PDMS solution into the Petri dish and perform the spin coating for 30 s at 1,000 rpm (**Figure 4c**).
3. Place the microchip surface that is going to be located on the microscope on the Petri dish (**Figure 4d**). Place the Petri dish in the oven for 1 h at 80 °C to solidify the PDMS solution.
4. Cut the border of the microchip and PDMS using a razor blade and subsequently detach it from the Petri dish (**Figures 4e, f**).

5. Laser Coupling to Insert the SMF Cable to the Microchip

NOTE: For the plasmonic tweezer system, an optical fiber incident laser with a 1,064-nm wavelength is used. The SMF cable is used because the diameter of the incident laser (5 mm) is too immense to emit the laser beam at the nanohole milled on the gold block (400 x 150 μm^2) in the microchip. The cladding diameter of the SMF cable is 125 µm. Thus, the incident laser and SMF cable must be coupled.

1. Connect a 40X objective lens to the microscope objective mount on the SMF coupler. Fix the SMF cable on the fiber clamp of the SMF coupler. Align the incident laser beam to fill in the back aperture of the objective lens.
2. Focus the laser beam to the core of the SMF cable by adjusting the three-axis manual stage equipped on the SMF coupler.
3. Insert the opposite end of the SMF cable into the SMF cable hole of the microchip. Measure the laser power prior to the insertion at the edge of the fiber cable, because the fixed fiber cable at the microchip cannot be detached.
4. Seal the SMF cable hole using epoxy glue to block the leakage of the flowing particle solution from the gap between the SMF cable hole (300 µm) and the cladding of the SMF cable (125 µm); the end of the inserted fiber cable should not enter the microchannel to avoid the fluid flow. Manually align the fiber cable using visual feedback so that it is perpendicular to the gold block that hosts the nanohole.

6. Plasmonic Trapping of Single Fluorescent Polystyrene Particle in the Microchip

1. Attach the syringe, which is filled with the particle solution, to a syringe micropump. Place the cover glass on the sample stage of the fluorescent microscope. Connect tubes to the inlet/outlet holes of the microchip. Place the PDMS-coated microchip surface on top of the cover glass.
2. Position the microchip orthogonally to the 60X water immersion objective lens by observing the inside of the channel with the camera installed on the fluorescent microscope. Use transparent tape to fix the microchip in place. Connect the inlet tube of the microchip with the syringe needle.
3. Insert the particle solution to the microchip by controlling the micropump at 20 µm/s. At this moment, confirm that the fluorescent particle can be observed well in the channel when the fluorescent lamp is turned on.
4. Wait until the particle solution exits from the outlet of the microchip. Set the speed to 3.4 µm/s.
5. Turn the laser source device so that it emits the laser into the nanohole; the fluorescent particle will be trapped at the rim of the nanohole.
6. Ramp the fluid speed in increments of 0.4 µm/s by controlling the micropump until the trapped particle escapes. Measure the fluid speed when the trapped particles escape. Obtain the maximal trapping force for each laser intensity using this measured fluid speed.

Representative Results

The fabrication process of the PDMS microchannel and nanohole gold plate is shown in **Figures 1** and **2**. The method to combine the two parts and the actual microchip is shown in **Figure 3**. The PDMS was cut to reveal the inside of the channel from the side of the microchip. However, it was difficult to observe the particles flowing in the channel because of the surface roughness of the cutting plane. Therefore, we introduced the PDMS coating method to solve this problem, as shown in **Figure 4**.

We observed 5-µm, flowing polystyrene particles in the microchip to confirm the effect of the PDMS coating. **Figure 5** shows the actual fabricated microchip and particles observed in the microchip using the microscope. **Figure 5a** and **c** are the before and after appearances of the microchip. **Figure 5b** and **d** are the magnified surfaces of each. **Figure 5e** shows blurred particles flowing, whereas **Figure 5f** shows that the edges of the particles are notably clear and that movements can be monitored. As above, the PDMS coating of the microchip surface is essential to the monitoring of trapped particles.

Figure 6 shows the 100-nm polystyrene particle undergoing plasmonic optical trapping by the plasmonic tweezer system. An SMF cable with a 0.14 numerical aperture (NA) was used. A tube was inserted at the inlet/outlet holes of the microchip channel. A micropump was used to insert and collect the 100-nm fluorescent polystyrene particle solution. To emphasize the interior appearance of the trapped particle by the plasmonic phenomenon, the dotted parts of **Figure 6a** have been enlarged as an inset, **Figure 6b**. The laser delivered by the SMF cable inserted in the microchip was emitted to the nanohole of the gold block, and the particle flowed from left to right. Movement was detected at the nanohole rim, where the field enhancement was the strongest.

Figure 7 shows consecutive images where a 100-nm fluorescent polystyrene particle that flowed in the microchannel was trapped and released at the nanohole at the intensity of 0.42 mW/μm^2. The particles flowed at a constant speed of 3.4 μm/s in the fluid direction, as shown in **Figure 7a**. After the laser was turned on, one of the particles was trapped at the nanohole, as shown in **Figure 7b**. On the contrary, another particle flowed into the stream, as shown in **Figure 7c**. Then, the flow speed was increased until the trapped particle escaped. **Figure 7d** shows the particle escaping from the trap. At this moment, we can estimate the trapping force with direct observation by measuring the fluid velocity when the particle escaped. We also worked in the opposite direction. Instead of increasing the fluid velocity, we gradually decreased the laser power in decrements of 1 mW and recorded the intensity when the particle escaped. This laser intensity is defined as the minimum trapping laser intensity and was measured to be 0.24 mW/μm^2.

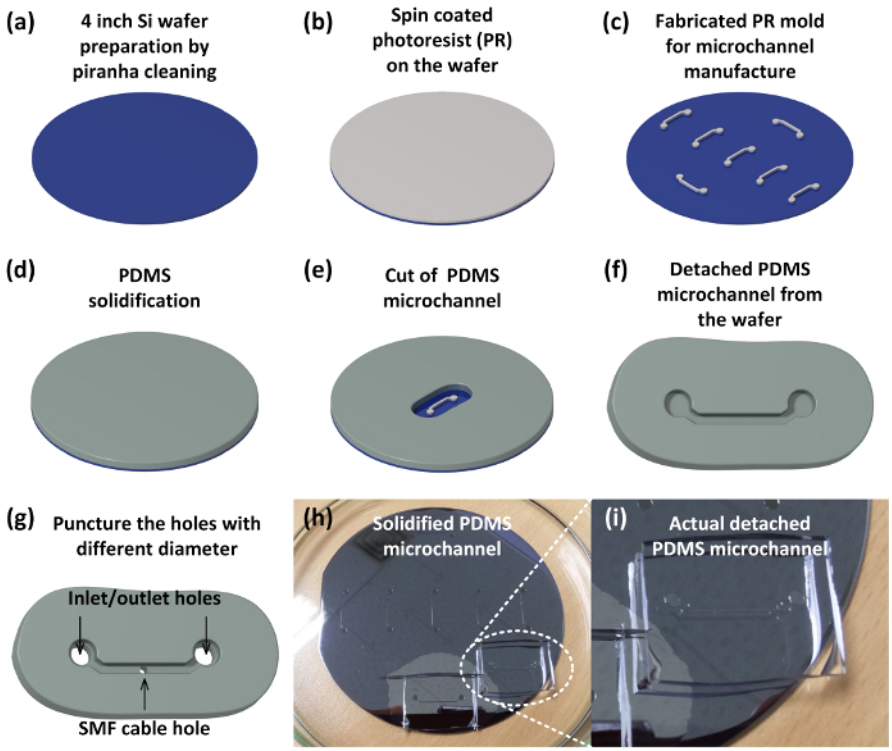

Figure 1. Fabrication of the PDMS microchannel. (**a**) Preparation of the Si wafer. (**b**) Photoresist spin coating of the wafer. (**c**) Fabricated microchannel mold by the photolithography process. (**d**) PDMS solidification using an oven after pouring the PDMS solution on the wafer. (**e**) PDMS microchannel cutting. (**f**) PDMS microchannel detachment from the wafer. (**g**) Inlet/outlet and SMF cable holes punctured on the PDMS microchannel. (**h**) Actual solidified PDMS on the wafer. (**i**) Actual detached PDMS microchannel. Please click here to view a larger version of this figure.

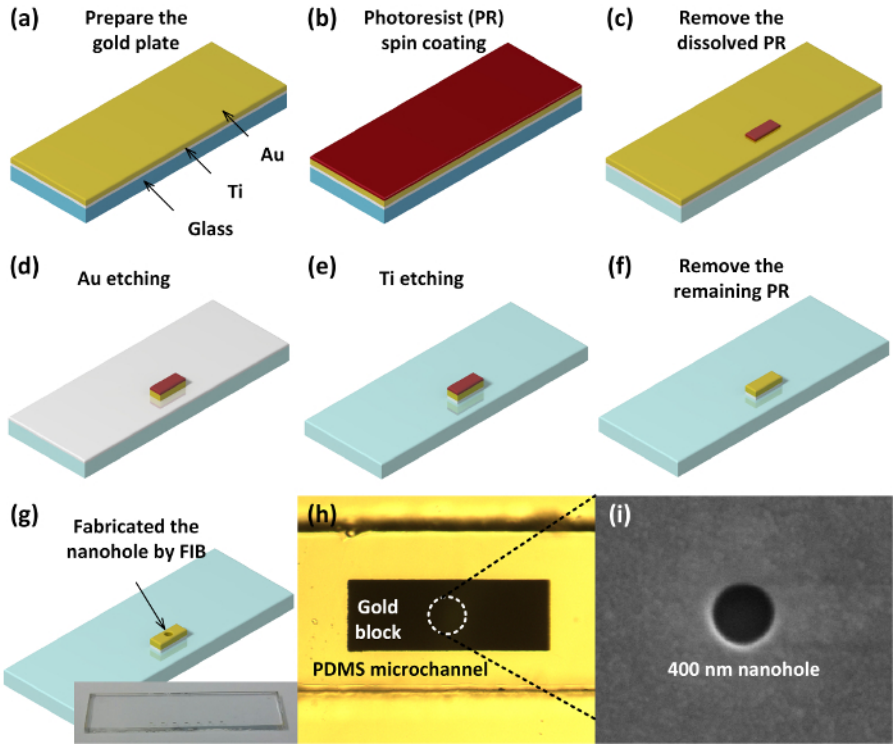

Figure 2. Fabrication of the nanohole on the gold plate after the etching process. (**a**) Deposition of Au and Ti on the glass. (**b**) Photoresist spin coating of the gold plate. (**c**) Dissolved photoresist removal after UV light exposure. (**d**) Au etching. (**e**) Ti etching. (**f**) Remaining photoresist removal. (**g**) Nanohole milling by a focused ion beam on the gold block. (**h**) Actual fabricated gold block. (**i**) Actual milled nanohole on the gold block. Please click here to view a larger version of this figure.

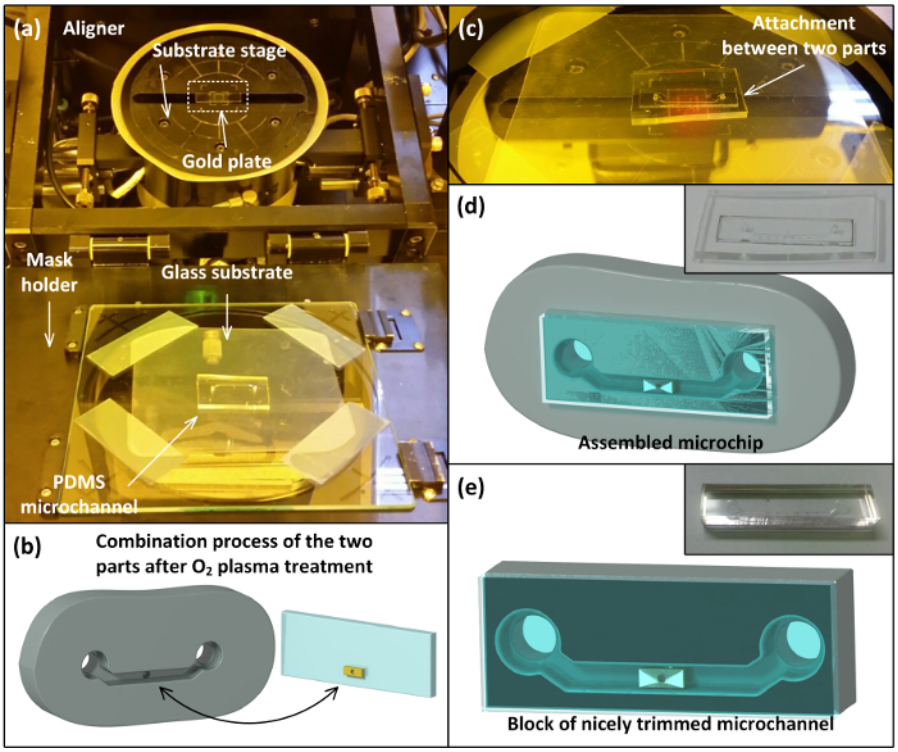

Figure 3. Assembly process of the microchip. (**a**) Fix the PDMS microchannel and gold plate on the mask holder and substrate stage, respectively, equipped on the aligner. (**b**) Combination of the PDMS microchannel part and the gold plate after surface treatment with O_2 plasma. (**c**, **d**) Assembled microchip after combination. (**e**) Removal of excess amount of the PDMS microchannel. Please click here to view a larger version of this figure.

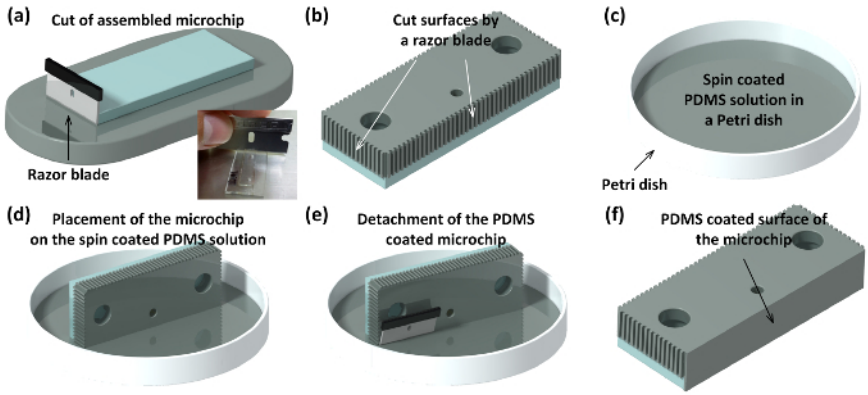

Figure 4. Process of surface roughness improvement by PDMS coating. (**a**) Remove excess amount using a razor blade after combining the two parts. (**b**) High surface roughness of the microchip after cutting. (**c**) PDMS solution spin coating in a Petri dish. (**d**) Dipping the window surface of the microchip into the spin-coated PDMS solution. (**e**) PDMS-coated microchip detachment from the Petri dish. (**f**) Improvement of surface roughness by PDMS coating. Please click here to view a larger version of this figure.

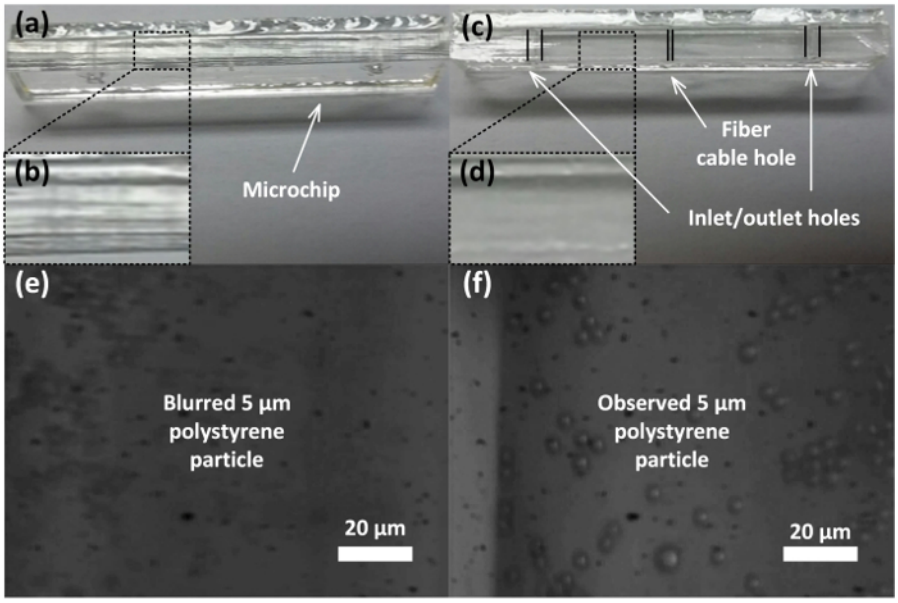

Figure 5. Assembled microchip and observation of 5-µm polystyrene particles in the microchannel before and after PDMS coating. (**a**, **b**) Microchip before PDMS coating and magnified view. (**c**, **d**) Microchip after PDMS coating and magnified view. (**e**, **f**) Observation of particles in the microchannel before and after PDMS coating. Please click here to view a larger version of this figure.

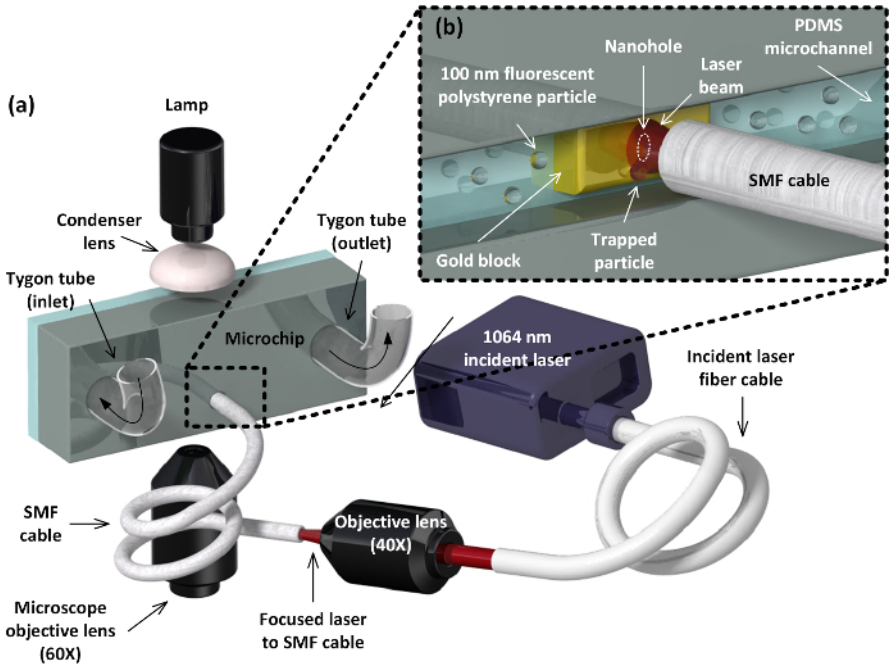

Figure 6. Designed plasmonic tweezer system. (**a**) Schematic of the plasmonic tweezer system. (**b**) Trapping of a 100-nm fluorescent polystyrene particle at the rim of the nanohole in the microchip. Please click here to view a larger version of this figure.

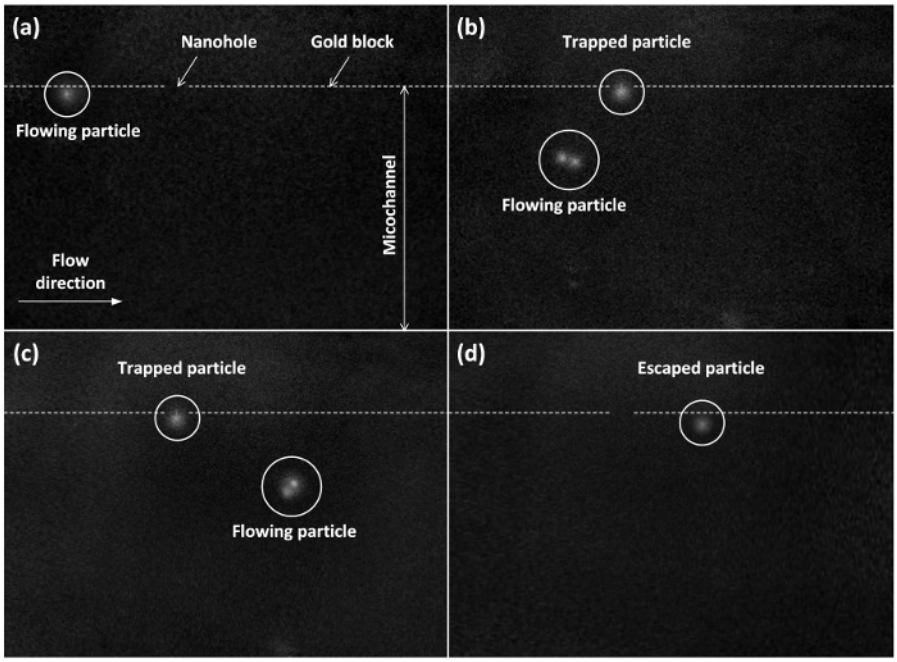

Figure 7. Trapping and releasing of a 100-nm fluorescent polystyrene particle in the microchannel. (**a**) The microchannel with a particle flowing into the stream. (**b**, **c**) Trapped particle at the nanohole compared to another particle. (**d**) Particle that escaped from the trap due to the increased fluid force. Please click here to view a larger version of this figure.

Discussion

The SMF cable was inserted in the SMF cable hole on the microchip, as shown in the rectangular dot of **Figure 6a**. Because the SMF cable hole is larger than the cable diameter, epoxy glue was used to seal the gap to block the leakage of the flowing particle solution. Before the application of epoxy glue, the gold block and cable edge should be coaxially aligned by hand using a microscope. Although it is ideal for the inserted cable edge and the nanohole to be coaxially aligned, a slight misalignment can be tolerated because the laser beam diverges once it is emitted from the end of the 0.14 NA SMF cable edge, and the beam affects a much larger region. Because the microchip was configured to be perpendicular to the optical axis of the microscope, we could not directly observe the location of the nanohole. The location of the nanohole

can only be indirectly determined by observing the location of the plasmonically trapped particle at the nanohole. A solution can be provided by installing a camera at the fiber cable and using it to monitor the gold block.

The distinctive feature of the microchip is its ability to monitor particle motion near the plasmonic nanohole in real time. The motion of the particle follows the scenario described below. When the fluid streams the particles forward, some particles move toward the gold block. In some cases, a particle gets notably close to the rim of the nanohole due to attraction to the nanohole and eventually becomes immobilized. At this moment, the optical force exerted on the particle exceeds the fluid force. Subsequently, the immobilized particle escapes from the nanohole rim when the fluid velocity increases; thus, the fluid force becomes stronger than the optical force. The maximal trapping force can be measured from this terminal fluid velocity. However, the conventional drag force equation cannot be used because the particle is in physical contact with the gold wall at the nanohole. To consider the surface effect of the gold wall, we used the finite-element method, which considers the fluid motion near the surface, and obtained the fluid force.

We have introduced a new plasmonic tweezer setup that enables the monitoring of particle dynamics along the laser beam axis. In contrast, previous studies have only introduced particle movement in the plane perpendicular to the laser beam axis, such as with the nanoblock[12], nanodisk[13,14,19,21], nanostick[20], and nanopyramid[18]. Furthermore, in the case of nanohole types, trapping can only be witnessed by monitoring the scattering signal, and not by visual monitoring[10,11,23]. However, we could not precisely measure the particle position because of the limited capabilities of current imaging techniques. The imaging quality should be further improved to confirm the exact dislocation measurements. This technique can be applied in the characterization and biosensing of a single molecule.

Disclosures

The authors have nothing to disclose.

Acknowledgements

This work was supported by the ICT R&D program of MSIP/IITP (R0190-15-2040, Development of a contents configuration management system and a simulator for 3D printing using smart materials).

References

1. Crane, N.B., Onen, O., Carballo, J., Ni, Q., Guldiken., R. Fluidic assembly at the microscale: progress and prospects. *Microfluid. Nanofluid.* **14**, 383-419 (2013).
2. Yao, B., Luo, G.-A., Feng, X., Wang, W., Chen, L.-X., Wang, Y.-M. A microfluidic device based on gravity and electric force driving for flow cytometry and fluorescence activated cell sorting. *Lab Chip* . **4**, 603-607 (2004).
3. Zhang, K., *et al.* On-chip manipulation of continuous picoliter-volume superparamagnetic droplets using a magnetic force. *Lab Chip.* **9**, 2992-2999 (2009).
4. Park, I.-Y., Sung, S.-Y., Lee, J.-H., Lee, Y.-G. Manufacturing micro-scale structures by an optical tweezers system controlled by five finger tips. *J. Micromech. Microeng.* **17**, N82-N89 (2007).
5. Kim, J.-D., Hwang, S.-U., Lee, Y.-G. Traceable assembly of microparts using optical tweezers. *J. Micromech. Microeng.* **22**, 105003 (2012).
6. Kim, J.-D., Lee, Y.-G. Construction and actuation of a microscopic gear assembly formed using optical tweezers. *J. Micromech. Microeng.* **23**, 065010 (2013).
7. Kim, J.-D., Choi, J.-H., Lee, Y.-G. A measurement of the maximal forces in plasmonic tweezers. *Nanotechnology.* **26**, 425203 (2015).
8. Kim, J.-D., Lee, Y.-G. Trapping of a single DNA molecule using nanoplasmonic structures for biosensor applications. *Biomed. Opt. Express.* **5**, 2471-2480 (2014).
9. Quidant, R. Plasmonic tweezers - the strength of surface plasmons. *MRS Bull.* **37**, 739-744 (2012).
10. Juan, M.L., Gordon, R., Pang, Y., Eftekhari, F., Quidant, R. Self-induced back-action optical trapping of dielectric nanoparticles. *Nat. Phys.* **5**, 915-919 (2009).
11. Pang, Y., Gordon, R. Optical trapping of 12 nm dielectric spheres using double-nanoholes in a gold film. *Nano Lett.* **11**, 3763-3767 (2011).
12. Tanaka, Y., Kaneda, S., Sasaki, K. Nanostructured potential of optical trapping using a plasmonic nanoblock pair. *Nano Lett.* **13**, 2146-2150 (2013).
13. Kang, J.-H., *et al.* Low-power nano-optical vortex trapping via plasmonic diabolo nanoantennas. *Nat. Commun.* **2**, 582 (2011).
14. Roxworthy, B.J., *et al.* Application of plasmonic bowtie nanoantenna arrays for optical trapping, stacking, and sorting. *Nano Lett.* **12**, 796-801 (2012).
15. Shoji, T., Tsuboi, Y. Plasmonic optical tweezers toward molecular manipulation: tailoring plasmonic nanostructure, light source, and resonant trapping. *J. Phys. Chem. Lett.* **5**, 2957-2967 (2014).
16. Pang, Y., Gordon, R. Optical trapping of a single protein. *Nano Lett.* **12**, 402-406 (2012).
17. Tsuboi, Y., *et al.* Optical trapping of quantum dots based on gap-mode-excitation of localized surface plasmon. *J. Phys. Chem. Lett.* **1**, 2327-2333 (2010).
18. Shoji, T., *et al.* Permanent fixing or reversible trapping and release of DNA micropatterns on a gold nanostructure using continuous-wave or femtosecond-pulsed near-infrared laser light. *J. Am. Chem. Soc.* **135**, 6643-6648 (2013).
19. Grigrenko, A.N., Roberts, N.W., Dickson, M.R., Zhang, Y. Nanometric optical tweezers based on nanostructured substrates. *Nat. Photonics.* **2**, 365-370 (2008).
20. Righini, M., *et al.* Nano-optical trapping of rayleigh particles and escherichia coli bacteria with resonant optical antennas. *Nano Lett.* **9**, 3387-3391 (2009).
21. Chen, K.-Y., Lee, A.-T., Hung, C.-C., Huang, J.-S., Yang, Y.-T. Transport and trapping in two-dimensional nanoscale plasmonic optical lattice. *Nano Lett.* **13**, 4118-4122 (2013).
22. Berthelot, J., *et al.* Three-dimensional manipulation with scanning near-field optical nanotweezers. *Nat. Nanotechnol.* **9**, 295-299 (2014).

23. Chen, C., *et al*. Enhanced optical trapping and arrangement of nano-objects in a plasmonic nanocavity. *Nano Lett.* **12**, 125-132 (2011).
24. Wang, K., Schonbrun, E., Steinvurzel, P., Crozier, K.B. Trapping and rotating nanoparticles using a plasmonic nano-tweezer with an integrated heat sink. *Nat. Commun.* **2**, 469 (2011).
25. Byun, D., Cho, S. J., Kim, S. Fabrication of a flexible penetrating microelectrode array for use on curved surfaces of neural tissues. *J. Micromech. Microeng.* **23**, 125010 (2013).

